Supporting Information for:

Atomically Resolving Polymorphs and Crystal Structures of In_2Se_3

Lixuan Liu[1,2#], Jiyu Dong[2#], Junquan Huang[2], Anmin Nie[2,*], Kun Zhai[2,*], Jianyong Xiang[2], Bochong Wang[2], Fusheng Wen[2], Congpu Mu[2], Zhisheng Zhao[2], Yongji Gong[1,*], Yongjun Tian[2], Zhongyuan Liu[2]

[1]*School of Materials Science and Engineering, Beihang University, Beijing 100191, China*
[2]*Center for High Pressure Science, State Key Lab of Metastable Materials Science and Technology, Yanshan University, Qinhuangdao 066004, China*

[#] *These authors contributed equally to the work.*

To whom correspondence should be addressed. E-mails: anmin@ysu.edu.cn, kunzhai@ysu.edu.cn, yongjigong@buaa.edu.cn

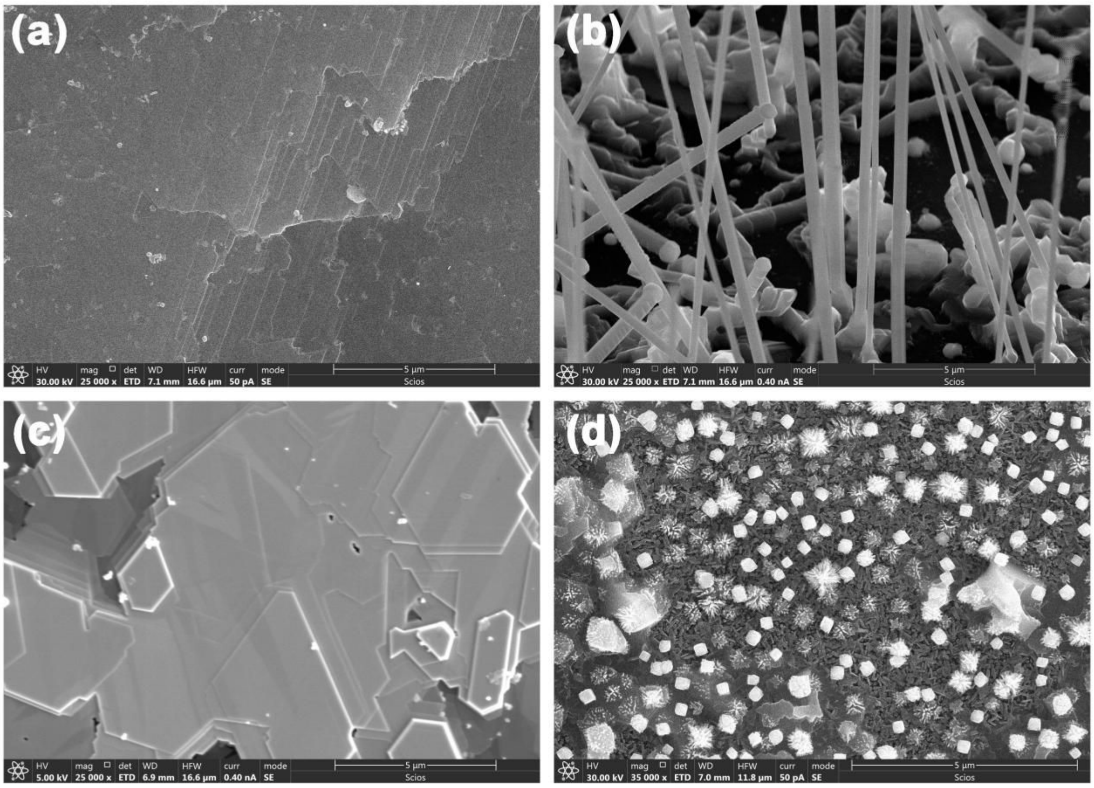

Figure S1 SEM images of In_2Se_3 grown on SiO_2/Si substrate (a), In_2Se_3 nanowirs (b), In_2Se_3 grown on HOPG substrate (c) and γ-In_2Se_3 (d).

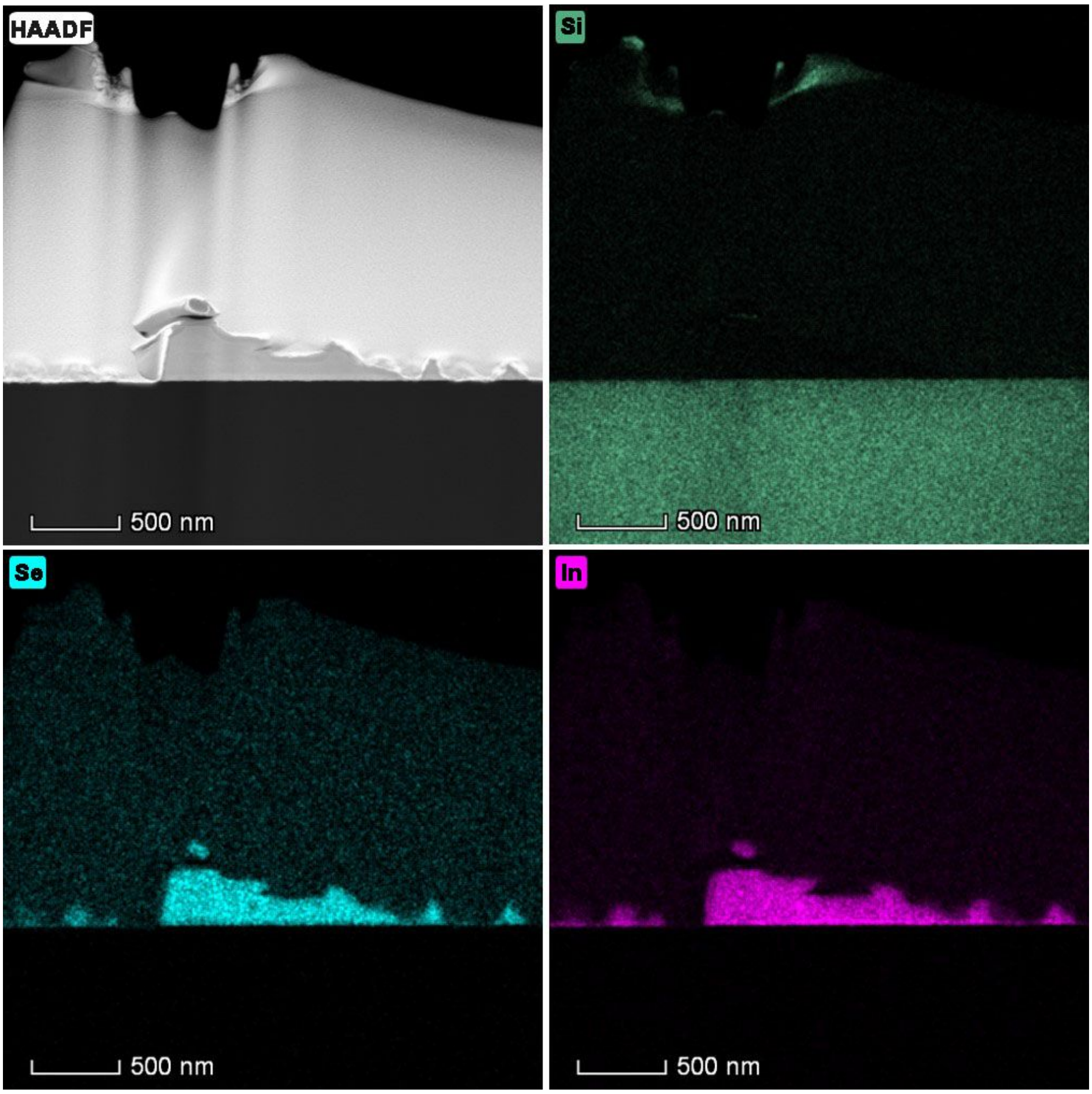

Figure S2 Cross-sectional HAADF and corresponding elemental EDX mapping of In2Se3 grown on SiO_2/Si substrate.

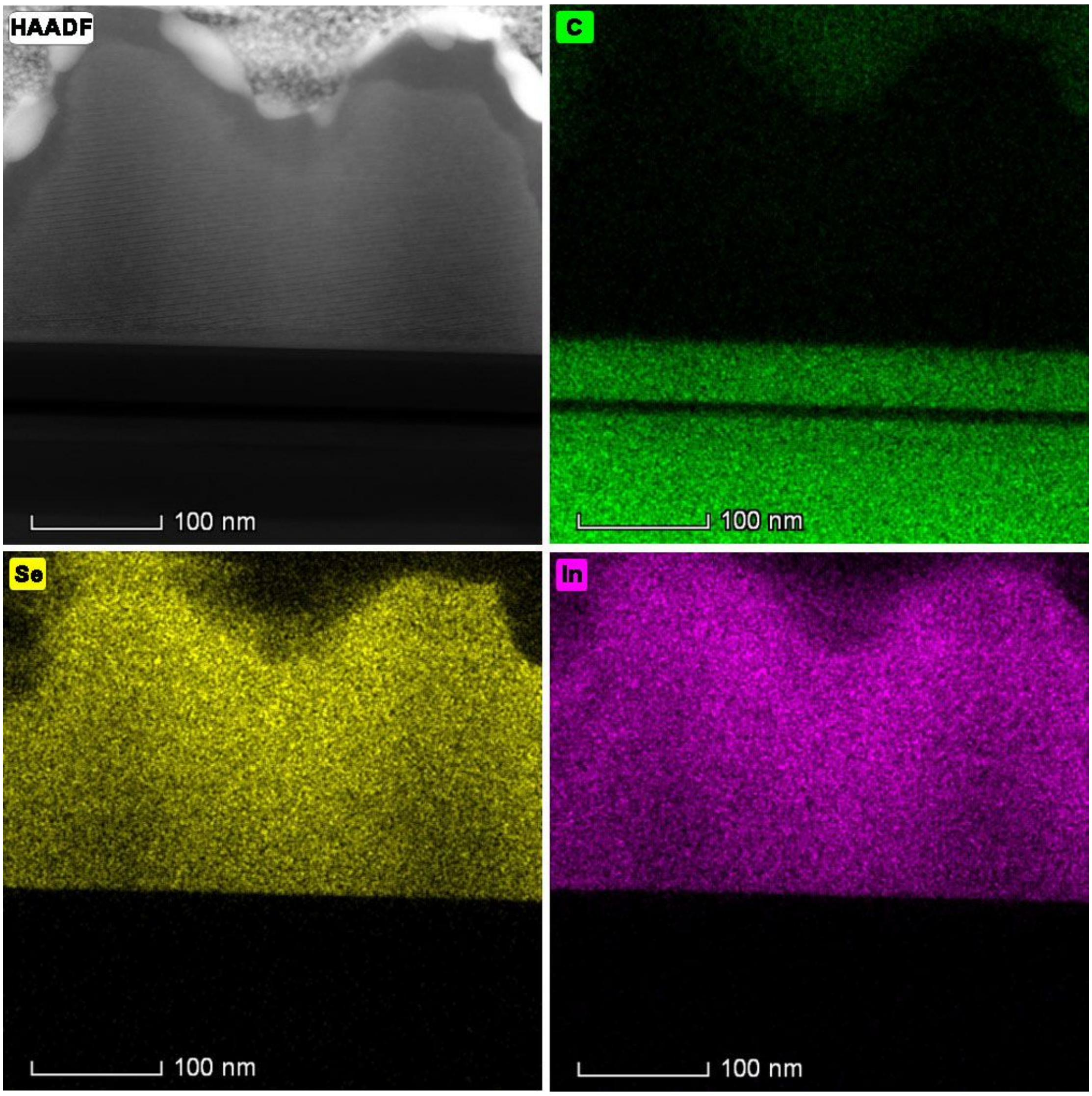

Figure S3 Cross-sectional HAADF and corresponding elemental EDX mapping of In2Se3 grown on HOPG substrate.

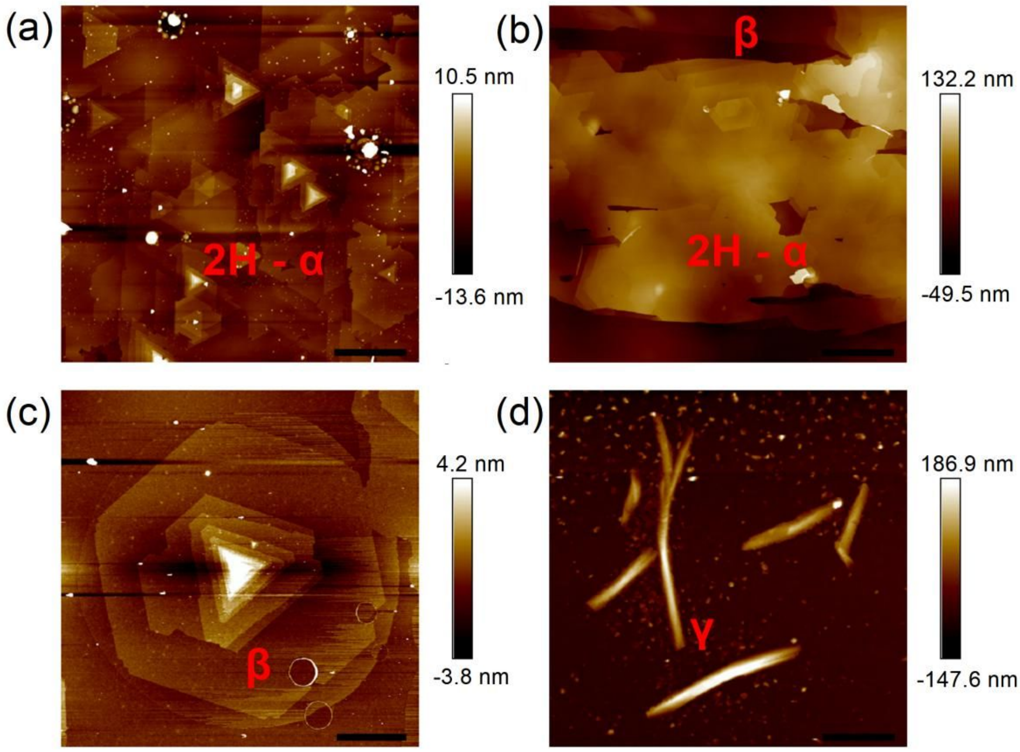

Figure S4 The AFM images of In_2Se_3 (a) In_2Se_3 crystal grown on SiO_2/Si substrate by CVD, which is co-exist of 2H-α, 3R, and 1T- β phases distinguished by TEM. (b) The AFM image of In_2Se_3 crystals grown on the HOPG substrate by CVD method. The mixed α and β- In_2Se_3 phases was observed in the domain. (c) The AFM image of β-In_2Se_3 grown on WS_2 substract presenting a circular shape in first layer and triangle shape in the subsequent layers. (d) The γ-In_2Se_3 grown on SiO_2/Si substrate, showing a needle-like shape. The scale bar in (a) - (d) is 2.0 μm, 5.0 μm, 6.0 μm and 4.0 μm, respectively.

Table S1 The crystal structure of different types of In_2Se_3

Polymorph	Crystal Structure	Space group	Lattic Parameters a (Å)	Lattic Parameters c (Å)	Reference
α-In_2Se_3	rhombohedral	*R3m*	4.05	29.64	This work
		R-3m	4.025	28.762	[1]
		R-3m	4.032	28.705	[2]
		R-3m	4.205	28.742	[3]
		R3m	4.026	28.75	[4]
		R3m	4.00	28.80	[11]
		R3m	4.05	28.77	[5]
		R3m	4.028	28.731	[6]
	hexagonal	*P63mc*	4.05	19.75	This work
		P63/mmc	4.025	19.235	[1]
		-	4.05	19.23	[7]
		P63mc	4.023	19.217	[4]
β-In_2Se_3	trigonal	*P-3ml*	4.04	9.76	This work
	hexagonal	*P63mc*	4.06	19.48	This work
		P63/mmc	4.0157	19.222	[8]
	rhombohedral	*R-3m*	4.000	28.33	[1]
		R-3m	3.832	25.16	[6]
		R-3m	4.166	28.213	[3]
γ-In_2Se_3	hexagonal	*P61*	7.35	20.02	This work
		P61 or P65	7.1286	19.381	[8]
		P61 or P65	7.17	19.41	[9]
		P61	7.13	19.38	[10]

Table S2 Summary of typical Raman peaks for α- β- β'- and γ-In_2Se_3

Polymorph	Crystal Structure	Crystal Preparation	Excitation Wavelength (nm)	Typical Raman Peaks (cm^{-1})				Ref.
				~90	~104	~180	~195	
α-In_2Se_3	hexagonal	growth by CVD on SiO2/Si wafer	532; 473; 633	√ 88	√	√ 179	√	This work
		exfoliation of bulk crystal from 2D Semiconductor	532	√	√	√	√	[12]
		exfoliation of bulk crystal from 2D Semiconductor	532	√	√	√	√	[13]
	rhombohedral	exfoliation of powder from Alfa Aesar; growth by VPD on mica; both annealed	488		√	√ 182		[14]
		grown by vertical gradient freezing method	488		√	√ 182		[15]
		grown by temperature gradient method	532		√ 107	√ 186	√ 196	[2]
			514.5	√ 95	√ 108	√ 185		[16]
		grown by CVD on mica	532		√ 108	√		[17]
		exfoliation of powder from Alfa Aesar	632		√ 108	√ 181		[3]
		grown by PVD on SiO2/Si wafer	532			√	√ 192	[18]
		grown by PVT on ε-GaSe substrate	532		105	√ 182	√ 187	[19]
		exfoliation of bulk crystal from Alfa Aesar	532	√ 91	√	√ 181		[17]
		exfoliation of bulk crystal from 2D Semiconductor	532			√ 181		[21]

	powder from Alfa Aesar	532	√ 89.2	√ 103.5	√ 182.3	√ 192.8	[6]

			Typical Raman Peaks (cm^{-1})			
			~110	~176	~205	
β-In_2Se_3	growth by CVD on SiO2/Si wafer	532; 473; 633	√ 109	√	√	This work
	annealing of the exfoliated α-In2Se3	633	√		√	[3]
	grown by PVT on ε-GaSe substrate	532	√	√ 175	√	[19]
	colloidal synthesis	514.5			√	[22]
	annealing of the exfoliated α-In2Se3	532	√	√	√ 207	[20]
	grown by PLD on Si wafer	533	√	√ 175	√ 208	[23]
β'-In_2Se_3	compresion of α-In2Se3 at room temperature	532	99.9	167.9	177.3	[6]

			Typical Raman Peaks (cm^{-1})			
			~150	~203	~228	
γ-In_2Se_3	growth by CVD on SiO2/Si wafer	532; 473; 633	√	√	√	This work
	grown by PVT on ε-GaSe substrate	532	√ 152	√ 205	√ 221	[19]
	grown by alternate thermal evaporation on soda lime glass substrate	1064	√	√ 205	√ 224	[10]

Reference:

[1] Popovic, S,; Tonejc, A.; Grzetaplenkovic, B.; Celustka, B.; Trojko, R. Revised and New Crystal Data for Indium Selenides. *J. Appl. Crystallogr.* **1979**, 12, 416.

[2] Nguyen, T. H.; Nguyen, V. Q.; Duong, A. T.; Cho, S. 2D semiconducting α-In_2Se_3 single crystals: Growth and huge anisotropy during transport. *J. Alloy. Compd.* **2019**, 810.

[3] Tao, X.; Gu, Y. Crystalline-crystalline phase transformation in two-dimensional In_2Se_3 thin layers. *Nano Lett.* **2013**, 13, 3501-5.

[4] Kupers, M.; Konze, P. M.; Meledin, A.; Mayer, J.; Englert, U.; Wuttig, M.; Dronskowski, R. Controlled Crystal Growth of Indium Selenide, In_2Se_3, and the Crystal Structures of alpha-In_2Se_3. *Inorg. Chem.* **2018**, 57, 11775-11781.

[5] Osamura, K.; Murakami, Y.; Tomiie, Y. Crystal Structures of αand β-Indium Selenide, In_2Se_3. *J. Phys. Soc. Jpn.* **1966**, 21, 1848−1848.

[6] Vilaplana, R.; Parra, S. G.; Jorge-Montero, A.; Rodriguez-Hernandez, P.; Munoz, A.; Errandonea, D.; Segura, A.; Manjon, F. J. Experimental and Theoretical Studies on alpha-In_2Se_3 at High Pressure. *Inorg. Chem.* **2018**, 57, 8241-8254.

[7] Jacobs-Gedrim, R. B.; Shanmugam, M.; Jain, N.; Duran, C. A.; Murphy, M. T.; Murray, T. M.; Matyi, R. J.; Moore, R. L. II.; Yu, B. Extraordinary Photoresponse in Two-Dimensional In_2Se_3 Naosheets. *ACS Nano* **2014**, 8, 514-521.

[8] Lutz, H. D.; Fischer, M.; Baldus, H.P.; Blachnik, R. Zur Polymorphie des In_2Se_3. *J. Less-Common Met.* **1988**, 143, 83-92.

[9] Vassilev, G. P.; Daouchi, B.; Record, M. C.; Tedenac, J. C. Thermodynamic Studies of the In-Se System. *J. Alloy. Compd*. **1998**, 269, 107-115.

[10] Marsillac, S.; Combot-Marie, A. M.; Bernede, J. C.; Conan, A. Experimental Evidence of the Low-Temperature Formation of γ-In_2Se_3 Thin Films Obtained by a Solid-State Reaction. *Thin Solid Films* **1996**, 288, 14-20.

[11] Ye, J. P.; Soeda, S.; Nakamura, Y.; Nittono, O. Crystal Structures and Phase Transformation in In_2Se_3 Compound Semiconductor. *Jpn. J. Appl. Phys*. **1998**, 37, 4264.

[12] Xue, F.; Hu, W.; Lee, K. C.; Lu, L. S.; Zhang, J.; Tang, H. L.; Han, A.; Hsu, W. T.; Tu, S.; Chang, W. H.; Lien, C. H.; He, J. H.; Zhang, Z.; Li, L. J.; Zhang, X. Room-Temperature Ferroelectricity in Hexagonally Layered α-In_2Se_3 Nanoflakes down to the Monolayer Limit. *Adv. Func. Mater.* **2018**, 28.

[13] Xue, F.; Zhang, J.; Hu, W.; Hsu, W. T.; Han, A.; Leung, S. F.; Huang, J. K.; Wan, Y.; Liu, S.; Zhang, J.; He, J. H.; Chang, W. H.; Wang, Z. L.; Zhang, X.; Li, L. J. Multidirection Piezoelectricity in Mono- and Multilayered Hexagonal alpha-In_2Se_3. *ACS Nano* **2018**, 12, 4976-4983.

[14] Zhou, Y.; Wu, D.; Zhu, Y.; Cho, Y.; He, Q.; Yang, X.; Herrera, K.; Chu, Z.; Han, Y.; Downer, M. C.; Peng, H.; Lai, K. Out-of-Plane Piezoelectricity and Ferroelectricity in Layered alpha-In_2Se_3 Nanoflakes. *Nano Lett.* **2017**, 17, 5508-5513.

[15] Lewandowska, R.; Bacewicz, R.; Filipowicz, J.; Paszkowicz, W. Raman Scattering in α-In_2Se_3 *Crystals. Mater. Res. Bull.* **2001**, 36, 2577.

[16] Kambas, K.; Julien, C.; Jouanne, M.; Likforman, A.; Guittard, M. Raman Spectra of α- and γ-In_2Se_3. *Phys. Stat. Sol. (b)*. **1984**, 124, K105.

[17] Feng, W.; Zheng, W.; Gao, F.; Chen, X.; Liu, G.; Hasan, T.; Cao, W.; Hu, P. Sensitive Electronic-Skin Strain Sensor Array Based on the Patterned Two-Dimensional α-In_2Se_3. *Chem. Mater.* **2016**, 28, 4278-4283.

[18] Zhou, J.; Zeng, Q.; Lv, D.; Sun, L.; Niu, L.; Fu, W.; Liu, F.; Shen, Z.; Jin, C.; Liu, Z. Controlled Synthesis of High-Quality Monolayered alpha-In_2Se_3 via Physical Vapor Deposition. *Nano Lett.* **2015,** 15, 6400-5.

[19] Balakrishnan, N.; Steer, E. D.; Smith, E. F.; Kudrynskyi, Z. R.; Kovalyuk, Z. D.; Eaves, L.; Patanè, A.; Beton, P. H. Epitaxial growth of γ-InSe and α, β, and γ-In_2Se_3 on ε-GaSe. *2D Materials* **2018**, 5.

[20] Feng, W.; Gao, F.; Hu, Y.; Dai, M.; Liu, H.; Wang, L.; Hu, P. Phase-Engineering-Driven Enhanced Electronic and Optoelectronic Performance of Multilayer In_2Se_3 Nanosheets. *ACS Appl. Mater. Interfaces* **2018**, 10, 27584-27588.

[21] Island, J. O.; Blanter, S. I.; Buscema, M.; van der Zant, H. S.; Castellanos-Gomez, A, Gate Controlled Photocurrent Generation Mechanisms in High-Gain In_2Se_2 Phototransistors. *Nano Lett.* **2015**, 15, 7853-8.

[22] Almeida, G.; Dogan, S.; Bertoni, G.; Giannini, C.; Gaspari, R.; Perissinotto, S.; Krahne, R.; Ghosh, S.; Manna, L. Colloidal Monolayer beta-In2Se3 Nanosheets with High Photoresponsivity. *J. Am. Chem. Soc.* **2017**, 139, 3005-3011.

[23] Zheng, Z.; Yao, J.; Wang, B.; Yang, Y.; Yang, G.; Li, J. Self-Assembly High-Performance UV-vis-NIR Broadband beta-In2Se3/Si Photodetector Array for Weak Signal Detection. *ACS Appl. Mater. Interfaces* **2017**, 9, 43830-43837.

[24] Han, G.; Chen, Z. G.; Drennan, J.; Zou, J. Indium selenides: structural characteristics, synthesis and their thermoelectric performances. *Small* **2014**, 10, 2747-65.

[25] Okamoto, H. In-Se (indium-selenium). *J. Phase. Equili. Diff.* **2004**, 25, 201-201.